Early extensional salt tectonics controls deep-water sediment dispersal

Davide Oppo[1], Christopher A-L Jackson[2], and Vittorio Maselli[3]

[1] Sedimentary Basins Research Group, School of Geosciences, University of Louisiana at Lafayette, Lafayette 70503, LA, US

[2] Landscapes and Basins Research Group (LBRG), Department of Earth Science & Engineering, Imperial College, Prince Consort Road, London, SW7 2BP, UK

[3] Università degli Studi di Modena e Reggio Emilia, Via Università 4, 41121, Modena, Italy.

ABSTRACT

The impact of seafloor deformation on sediment routing during the initial phases of extensional salt tectonics is largely unresolved despite influencing the volume of coarse-grained clastic material delivered to the deep sea. Using 3D seismic reflection data from the northern Levant Basin offshore Lebanon, we investigate the interplay between early extension-related salt deformation and deep-water sediment dispersal. Our results indicate that slope-parallel faults favor early sediment transfer to the abyssal plain. In contrast, slope-normal faults and ramp-syncline basins create significant accommodation, trapping deep-water channels at the base-of-slope and delaying coarse sediment transfer to the abyssal plain. These results help refine source-to-sink models of turbidite systems developing in young salt basins and highlight the crucial role of extensional tectonics in the early stages of basin development, emphasizing the impact of fault strike, ramp-syncline basin evolution, and salt welding on deep-water sediment routing. Our study increases the understanding of sediment transfer in young, evolving salt basins and has significant implications for predicting deep-water stratigraphy in mature, more structurally complex basins.

INTRODUCTION

Determining how deep-water sediment dispersal systems interact with seafloor structures is key to understanding how, how much, and where sediment is trapped along continental margins or, conversely, delivered to ocean basins. For example, several studies have investigated how salt-induced deformation and sediment gravity currents, such as turbidity currents and debris flows, interact with seabed structures to build deep-water channels and lobes (e.g., Loncke et al., 2006; Gee and Gawthorpe, 2006; Oluboyo et al., 2014; Howlett et al., 2021). These studies have typically focused on the distal, contraction-dominated parts of mature salt-tectonic systems (e.g., circum-Gulf of Mexico, offshore eastern Canada, circum-South Atlantic). In contrast, the impact of seafloor deformation during the initial phases of salt tectonics in the updip, extension-dominated zone has, to our knowledge, very rarely been documented. A notable exception is the study by Anderson et al. (2000), who show that long-term (c. 12 Myr) changes in fault-sediment interactions offshore Angola reflect gross variations in (salt-detached) fault-driven accommodation vs. sediment accumulation rate. These variations are expressed as an overall decrease in confinement, principally driven by an increase in sediment supply. Such interactions, in addition to ramp-syncline basins (RSB), a relatively common type of salt-related depocentre that forms slightly downdip of the extensional zone (e.g., Pichel et al., 2018), are not captured in generic models illustrating salt-sediment interactions on salt-detached slopes (e.g., Oluboyo et al., 2014; Cumberpatch et al., 2021; Howlett et al., 2021).

In contrast to most salt-influenced sedimentary basins, salt in the Mediterranean Sea is relatively young (<6 Myr), and, as a result, it and its relatively seismically well-imaged overburden have yet to experience intense deformation. We therefore use 3D seismic reflection data from the northern Levant Basin, eastern Mediterranean, to investigate the relationship between early extension-related, salt-tectonic deformation, and deep-water sediment dispersal, thereby helping refine source-to-sink models of salt-controlled depositional systems. This is particularly useful when trying to predict deep-water stratigraphy in more strongly deformed and/or deeply buried salt basins, where data may be sparse and/or seismic reflection imaging poor.

GEOLOGICAL SETTING

The Miocene to recent stratigraphy of the Levant Basin comprises evaporites (Messinian Salt) capped by up to 2 km of predominantly deep-water clastic deposits (e.g., Kabir et al., 2022; Oppo et al., 2023). Messinian Salt and its overburden were moderately deformed in response to westward gravity gliding induced by post-Pleistocene tilting and uplift of the northern Levantine margin (Cartwright and Jackson, 2008). Salt-detached gliding produced kinematically linked zones of updip extension and downslope contraction. Our study area is located in the updip extensional zone, which is dominated by reactive diapirism associated with predominantly N-S-striking, basinward-dipping, and salt-detached normal faults, some of which are expressed on the present seafloor. Margin-normal (i.e., E-trending) reactive diapirs and associated salt-detached faults are also observed, in addition to ramp-syncline basins (Fig. 1) (Evans et al., 2021).

The post-Messinian deep-water stratigraphy in the North Levant Basin has, to the best of our knowledge, only been described by Maselli et al. (2021), who investigated the spatial and temporal evolution of bedforms in a single, near-seabed (i.e., Recent) deep-water lobe cut by a salt-detached normal fault. They highlighted that extensional salt tectonics has had and likely continues to play a key role in controlling deep-water sedimentation and stratigraphic development.

DATA AND METHODS

We use 3D time-migrated seismic reflection data that is near-zero phase at the seafloor reflection and is displayed here with SEG negative polarity, i.e., downward increase and decrease in acoustic impedance are represented by a trough (blue in our seismic displays) and peak (red in our seismic displays) reflection, respectively (Brown, 2001). The dominant frequency in the post-salt overburden, extracted directly from the seismic dataset, is 50 Hz, with an average P-wave velocity of 2,000 m/s indicated by proprietary processing reports. Based on these data, the estimated vertical resolution for the post-salt overburden is ~10 m. The horizontal resolution is ~25 m, approximated as a quarter of the dominant wavelength

(Lebedeva-Ivanova et al., 2018). As shown below, these data are of sufficient quality to image the main salt-tectonic structures and the key depositional elements in the overburden.

The lack of well data offshore Lebanon prevents a precise calibration of the lithology and age of the overburden. We therefore use seismic facies analysis and the amplitude root mean square (RMS) to infer depositional system types and sediment grain size. More specifically, following Maselli et al. (2021) and other studies of deep-water seismic geomorphology (e.g., Prather et al., 1998), we interpret high RMS values as representing coarser, likely sand-rich sediment. The only absolute age is provided by the 1.8 Ma reflection, correlated from Oppo et al. (2021). However, the excellent seismic data quality means we can confidently establish a robust seismic-stratigraphic framework to define the relative if not absolute age of various depositional elements.

RESULTS

In the south of the study area, coarse sediment delivered from the shelf to the slope feeds a submarine channel (Channel A) (Fig. 1). This channel extends from the base-of-slope to the abyssal plain, crossing the extensional zone, where it is confined laterally by margin-normal and -oblique faults (Fig.1). In the easternmost, most proximal part of the survey, Channel A is underlain by stacked paleochannels, indicating it is a relatively long-lived system with the oldest paleochannels developed at ca. 1.8 Ma (Fig. 2A). Less than 5 km basinward, the stacked paleochannels disappear from the stratigraphy, and only the seabed expression of Channel A is present (Fig. 2B). Stacked paleochannels are also absent throughout the extensional zone, where the channel stratigraphy is mainly formed by high-amplitude, variable continuity seismic reflections, which are locally preserved within grabens (Figs. 3A, B).

Upon reaching the abyssal plain, Channel A encounters a RSB, where it incises a lobe defined by sheet-like, high-amplitude reflections. Notably, in this location, Channel A is defined by relatively low-amplitude reflections, suggesting it is finer-grained than its encasing lobe (Figs. 2E, 3C). Further basinward, the channel encounters a second RSB (Fig. 2C, E), where at least two stacked lobes, larger than the one in the updip RSB, occur. Like those in the updip RSB, these lobes are defined by high-amplitude reflections and are incised by a low-amplitude Channel A. Once it exits the second RSB, the channel becomes less confined, with the underlying stratigraphy being defined by well-developed, reflective, presumably sandy paleochannels. The stratigraphic relationship between the 1.8 Ma reflection and lobes in the downdip RSB/abyssal plain suggests that the onset of sandy deposition was broadly coincident with the initiation of the oldest paleo-channel observed in the most proximal part of the survey (Fig. 2A).

A second channel (Channel B) is present c. 8.6 km north of Channel A. Channel B shares many similarities with Channel A, i.e., it extends from the base-of-slope to the abyssal plain, crossing the salt-detached extensional zone (Fig. 1), and proximal to the base-of-slope is underlain by stacked paleochannels that developed after ca. 1.8 Ma (Fig. 2A), but which are absent from the stratigraphy immediately basinward of the first margin-parallel, salt-related graben (Fig. 2B). Unlike Channel A, however, Channel B is not laterally confined by faults at the base-of-slope, where it instead trends slope-parallel. Further downslope, in the central, more heavily faulted area, the channel abruptly turns 90° northward upon entering a margin-parallel graben, and then 90° westward, where it exits the graben before passing onto the abyssal plain and becoming relatively sinuous. Seismic sections across this tract of the channel show that it has an erosional base and is underfilled (Fig. 3D). On the abyssal plain, downslope of the extensional zone, Channel B has a moderately erosional base and is bounded by small levees (Fig. 2D), before passing downslope into at-seabed (i.e., Recent) lobes (Figs. 1C, 3D).

INTERPRETATION

Our data suggests early salt deformation in the extensional zone of a salt-detached slope controlled the sequestration and routing of deep-water sediment and the ultimate stratigraphic evolution of related channels and lobes. We interpret two main styles of salt-sediment interaction: (1) early and sustained delivery of coarse-grained sediment to the abyssal plain (as exemplified by Channel A), and (2) initial sequestration of sediment at the base-of-slope, with subsequent bypass of the extensional zone (as exemplified by Channel B).

Channel A – Early delivery to the abyssal plain

The stratigraphic relationship between the paleochannels, the downslope paleo-lobes, and the 1.8 Ma reflection indicates that coarse-grained sediment supply to the abyssal plain was established in the Early Pleistocene. Time-equivalent paleochannels at the base-of-slope and on the abyssal plain indicate that Channel A connected these two areas despite the lack of obvious paleochannel-related incisions across the extensional zone. We interpret that the apparent absence of incision reflects the combined effects of structural confinement by margin-normal and -oblique faults and related grabens, and the elevated sediment supply, which together caused channel filling, inhibited erosion, and aided basinward propagation of the channel. As a result, large volumes of coarse sediment were delivered through the extension zone directly to lobes on the abyssal plain.

Notably, however, upon reaching the abyssal plain, salt-detached translation still influenced sedimentation patterns, with RSBs temporarily providing accommodation for the local preservation of lobes. More specifically, we infer that the deposition of a sandy lobe in the updip RSB was followed by channel incision and coarse sediment bypass to the downdip RSB, where a stacked set of sandy lobes were deposited before the channel was filled by finer-grained material. These lobes were then incised by their feeder channel, which propagated basinward, feeding sandy material to the most distal part of the abyssal plain. The channel was ultimately filled by finer-grained material. The depositional patterns described here are comparable to those captured in deep-water fill-and-spill systems, where the relationship between accommodation and sediment accumulation rates controls depocenter filling vs. bypass. In this example, salt-detached translation, rather than minibasin subsidence (e.g., Prather et al., 1998) or contractional growth folding (e.g., Smith, 2004), caused the local development of intra-slope accommodation. Given that thick, stacked lobe-dominated successions are not preserved in the RSBs and that an overall fill-and-spill pattern is recorded, we suggest that RSB translation and subsidence rate were low relative to sediment supply.

Channel B – Early sequestration at the base-of-slope

Based on their stratigraphic relationship to the 1.8 Ma reflection, we infer the paleochannels associated with Channel B also initiated in the Early Pleistocene, at broadly the same time as Channel A. However, the lack of paleochannels, paleo-lobes, and other stratigraphic evidence of coarse-grained sediment delivery to, or at least preservation within, the extension zone and abyssal plain indicates that Channel B did not reach the deeper basin until relatively recently. This indicates that the most proximal margin-parallel, intra-slope graben efficiently trapped coarse-grained sediment, stopping it from reaching the base-of-slope and abyssal plain. Like Channel A, the depositional patterns described here are comparable to those captured in deep-water fill-and-spill models. Critically, however, at least during the earliest phase of development of Channel B, we only observe the ‘fill’ phase.

Over time, Channel B migrated southwards, beyond the southern limit of the graben (Fig. 2A). This, possibly coupled with slower subsidence and accommodation development rate due to progressive salt welding, allowed the channel to ultimately escape from the graben and extend basinward. However, the channel was eventually (and continues to be) partly confined by the next downslope graben. Within this new depocentre, the strongly erosional character of the channel (Fig. 3D) suggests that confinement favored (and perhaps still favors) sediment bypass through the entire upper course of the channel.

CONCLUSION AND IMPLICATIONS

Our study shows that extensional tectonics during the early stages of salt-detached extension controls sediment routing to the abyssal plain. More specifically, slope-parallel faults favor early sediment transfer through the extensional zone to the abyssal plain, whereas slope-normal faults and ramp-syncline basins generate considerable accommodation, thus favoring trapping and deflection of deep-water channels and the accumulation of coarse sediment at the base-of-slope. In the latter case, lateral channel migration and/or the cessation of accommodation generation due to salt welding meant that the channel could eventually transfer sediment toward and onto the abyssal plain. Our study highlights that fault strike relative to sediment input direction, RSB development and evolution, and the temporal relationship between sediment input and salt welding all need to be captured in tectono-stratigraphic models for salt basins, given these dictate if and where land-derived material is delivered to the deep ocean. Our results also provide insights into early-stage, deep-water stratigraphic patterns in salt basins that are now strongly deformed in response to ongoing tectonics.

ACKNOWLEDGMENTS

We acknowledge W. Chbat and the Lebanese Petroleum Administration for providing data; Schlumberger for granting Petrel© academic licenses.

REFERENCES CITED

Anderson, J.E., Cartwright, J., Drysdall, S.J., and Vivian, N., 2000, Controls on turbidite sand deposition during gravity-driven extension of a passive margin: examples from Miocene sediments in Block 4, Angola: Marine and Petroleum Geology, v. 17, p. 1165–1203, doi:10.1016/S0264-8172(00)00059-3.

Brown, A.R., 2001, Color in seismic display: The Leading Edge, v. 20, p. 549–549, doi:10.1190/1.1438992.

Cartwright, J.A., and Jackson, M.P.A., 2008, Initiation of gravitational collapse of an evaporite basin margin: The Messinian saline giant, Levant Basin, eastern Mediterranean: Geological Society of America Bulletin, v. 120, p. 399–413, doi:10.1130/B26081X.1.

Cumberpatch, Z.A., Kane, I.A., Soutter, E.L., Hodgson, D.M., Jackson, C.A.-L., Kilhams, B.A., and Poprawski, Y., 2021, Interactions between deep-water gravity flows and active salt tectonics: Journal of Sedimentary Research, v. 91, p. 34–65, doi:10.2110/jsr.2020.047.

Evans, S.L., Jackson, C.A.-L., and Oppo, D., 2021, Taking the Pulse of Salt-Detached Gravity Gliding in the Eastern Mediterranean: Tectonics, v. 40, p. e2020TC006476, doi:https://doi.org/10.1029/2020TC006476.

Gee, M.J.R., and Gawthorpe, R.L., 2006, Submarine channels controlled by salt tectonics: Examples from 3D seismic data offshore Angola: Marine and Petroleum Geology, v. 23, p. 443–458, doi:10.1016/j.marpetgeo.2006.01.002.

Howlett, D.M., Gawthorpe, R.L., Ge, Z., Rotevatn, A., and Jackson, C.A.-L., 2021, Turbidites, topography and tectonics: Evolution of submarine channel-lobe systems in the salt-influenced Kwanza Basin, offshore Angola: Basin Research, v. 33, p. 1076–1110, doi:10.1111/bre.12506.

Kabir, S.M.M., Iacopini, D., Hartley, A., Maselli, V., and Oppo, D., 2022, Seismic characterization and depositional significance of the Nahr Menashe deposits: Implications for the terminal phases of the Messinian salinity crisis in the north-east Levant Basin, offshore Lebanon: Basin Research, v. 00, p. 1–26, doi:10.1111/bre.12697.

Lebedeva-Ivanova, N., Polteau, S., Bellwald, B., Planke, S., Berndt, C., and Henriksen Stokke, H., 2018, Toward one-meter resolution in 3D seismic: The Leading Edge, v. 37, p. 794–864, doi:https://doi.org/10.1190/tle37110818.1.

Loncke, L., Gaullier, V., Mascle, J., Vendeville, B., and Camera, L., 2006, The Nile deep-sea fan: An example of interacting sedimentation, salt tectonics, and inherited subsalt paleotopographic features: Marine and Petroleum Geology, v. 23, p. 297–315, doi:10.1016/j.marpetgeo.2006.01.001.

Maselli, V., Micallef, A., Normandeau, A., Oppo, D., Iacopini, D., Green, A., and Ge, Z., 2021, Active faulting controls bedform development on a deep-water fan: Geology, v. 49, p. 1495–1500, doi:10.1130/G49206.1.

Oluboyo, A.P., Gawthorpe, R.L., Bakke, K., and Hadler-Jacobsen, F., 2014, Salt tectonic controls on deep-water turbidite depositional systems: Miocene, southwestern Lower Congo Basin, offshore Angola: Basin Research, v. 26, p. 597–620, doi:10.1111/bre.12051.

Oppo, D., Evans, S., Iacopini, D., Kabir, S.M., Maselli, V., and Jackson, C.A.-L., 2021, Leaky salt: pipe trails record the history of cross-evaporite fluid escape in the northern Levant Basin, Eastern Mediterranean: Basin Research, v. 33, p. 1798–1819, doi:https://doi.org/10.1111/bre.12536.

Oppo, D., Jackson, C.A.-L., Gorini, C., Iacopini, D., Evans, S., and Maselli, V., 2023, Mass wasting records the first stages of the Messinian Salinity Crisis in the eastern Mediterranean: Geology, v. 51, p. 637–641, doi:10.1130/G51146.1.

Pichel, L.M., Peel, F., Jackson, C.A.-L., and Huuse, M., 2018, Geometry and kinematics of salt-detached ramp syncline basins: Journal of Structural Geology, v. 115, p. 208–230, doi:10.1016/j.jsg.2018.07.016.

Prather, B.E., Booth, J.R., Steffens, G.S., and Craig, P.A., 1998, Classification, Lithologic Calibration, and Stratigraphic Succession of Seismic Facies of Intraslope Basins, Deep-Water Gulf of Mexico1: AAPG Bulletin, v. 82, p. 701–728, doi:10.1306/1D9BC5D9-172D-11D7-8645000102C1865D.

Smith, R., 2004, Silled sub-basins to connected tortuous corridors: sediment distribution systems on topographically complex sub-aqueous slopes, *in* Lomas, S.A. and Joseph, P. eds., Confined Turbidite Systems, Geological Society of London, v. 222, p. 0, doi:10.1144/GSL.SP.2004.222.01.03.

FIGURE CAPTIONS

Figure 1. (A) and (C) show the bathymetry of the study area using the variance and amplitude RMS seismic attributes, respectively. (B) Structural map showing the two channels (red), normal faults (black), and salt diapirs (pink). (C) The red/yellow color represents higher concentrations of coarse-grained sediment. (D) Seismic section shows the overall margin setting. Red faults are late to post-Messinian and are related to salt gliding toward the basin. Pink shading: Messinian Salt. RSB: Ramp syncline basin. RMS: Root Mean Square.

Figure 2. (A) to (D): Seismic profiles parallel to the margin (location in Fig. 1C) showing the channels evolution moving from the base-of-slope (A) to the abyssal plain (C-D). (E) RMS amplitude was calculated on the 1.8 Ma horizon in (C), showing two deep-sea lobes mainly formed by the deposition of coarse-grained sediment within two consecutive RSBs. Note the low amplitude of the channel incising the distal lobe. The dashed line delimits the RSB. Faults are red, Messinian Salt is pink, and sand-rich channels and lobes deposit in yellow.

Figure 3. Seismic cross-sections showing the lack of a well-developed Channel A incision within grabens (A) and half-grabens (B) across the extensional zone. (C) Well-developed paleochannels and deep-sea lobes are associated with Channel A within the first RSB (Fig. 2E for location). (D) Section parallel to the margin showing the erosional character of Channel B within a graben. Black arrows mark strata truncation. Flow within the channel is northeastwards. (E) Distal deep-sea lobes associated with Channel B. Note the low amplitude of the channel compared to the lobe. Faults are red, Messinian Salt is pink, and sand-rich channels and lobe deposits are yellow.

[1] Supplemental Material. The uninterpreted version of the seismic data showed in the manuscript. Please visit https://doi.org/10.1130/XXXX to access the supplemental material, and contact editing@geosociety.org with any questions.


Europe
Study area
Africa
Channel B
Channel A
Variance
min
max
34°00'N
33°48'N
35°00'E
35°20'E
A
2 km
N
Salt diapirs
Margin-parallel grabens
Channel B
Channel A
Deep-sea lobes
Margin-normal grabens
B
Fig. 2D
Fig. 3E
Fig. 2B
Fig. 2A
Fig. 2E
Fig. 3D
Fig. 1D
Fig. 3A
Fig. 3B
Fig. 2C
Fig. 3C
RMS
75k
0
C
W
E
Contractional domain
Extensional domain
RSB
RSB
Margin-parallel graben
Deep-sea lobe deposits
1.8 Ma
1.8 Ma
Salt diapir
Base-salt step
Base-salt step
Amplitude
-
+
1km
200ms
D


SW
Channel A
Channel B
NE
Graben
1.8 Ma
A
250ms
1km
SW
Channel A
Channel B
NE
Graben
B
250ms
1km
Channel A
SW
NE
1.8 Ma
Deep-sea
lobes
C
300ms
1km
Channel B
SW
NE
D
100ms
500m
Amplitude
-
+
RMS
Max
Min
N
Fig. 2C
RSBs
Channel
Deep-sea
lobes
Fig. 3C
E

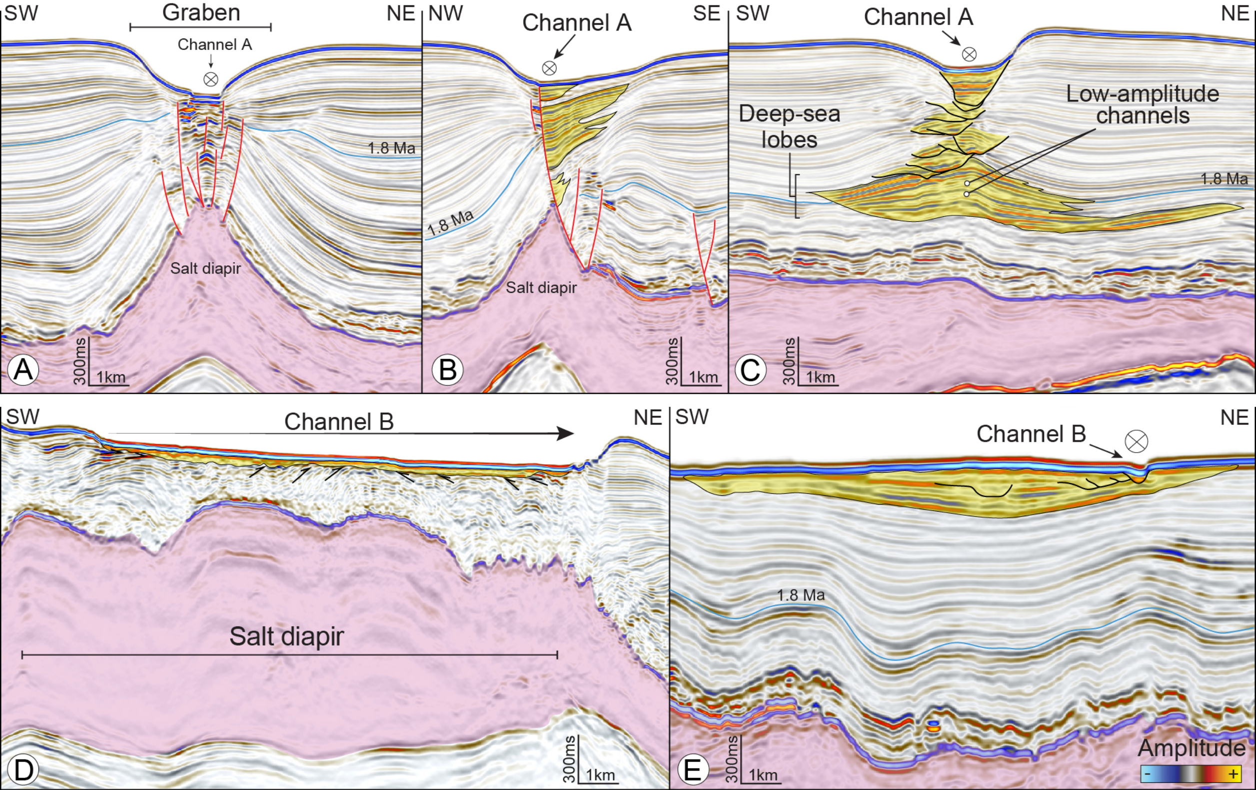
SW
Graben
NE
Channel A
1.8 Ma
Salt diapir
300ms
1km
A
NW
Channel A
SE
1.8 Ma
Salt diapir
300ms
1km
B
SW
Channel A
NE
Low-amplitude
channels
Deep-sea
lobes
1.8 Ma
300ms
1km
C
SW
Channel B
NE
Salt diapir
300ms
1km
D
SW
Channel B
NE
1.8 Ma
300ms
1km
E
Amplitude
-
+